XIV International Conference on Computational Plasticity. Fundamentals and Applications
COMPLAS 2017
E. Oñate, D.R.J. Owen, D. Peric and M. Chiumenti (Eds)

BOUNDED RATE DAMAGE PLASTIC MODEL FOR CONCRETE FAILURE UNDER IMPULSIVE LOADINGS

DANIEL GUILBAUD[*a,b]

* a DEN-Service d'études mécaniques et thermiques (SEMT), CEA, Université Paris-Saclay,
F-91191, Gif-sur-Yvette, France
* b IMSIA, EDF, CEA, CNRS, ENSTA Paris Tech, Université Paris Saclay,
828 Boulevard des Maréchaux, 91762 Palaiseau Cedex, France
e-mail: daniel.guilbaud@cea.fr

Key words: Concrete, Damage, Bounded rate, Mesh objectivity.

1 INTRODUCTION

This paper deals with the objective prediction of cracks in concrete structures within the framework of a local constitutive model. To reach this goal, it is necessary to overcome mesh dependency due to the softening of concrete. The constitutive law for concrete is an isotropic damage plastic model already described in [1]. The model has been introduced in EUROPLEXUS, a general finite element explicit code for fast transient analysis. The Hilleborg method used to maintain constant fracture energy regardless of element size is not able to deal with mesh-induced directional bias. In some cases, this leads to wrong failure mechanisms of the structure and to false ultimate load. Non-local models by their implicit nature are not adapted to explicit code and adversely affect its performance. This is the reason why the bounded rate concept presented in [2] has been introduced in the model. From a physical point of view, the basic idea is that the damage rate is finite because the cracking velocity is not instantaneous and from a mathematical point of view it was demonstrated in [2] that the problem remains well posed as long as damage rate is bounded and the damage not too close to 1.

After a short theoretical overview of the model, numerical implementation and calibration procedure are succinctly described, and then comparisons with tests are presented.

2 THEORETICAL OVERVIEW

The DPDC model belongs to the wide family of phenomenological concrete models. It is an isotropic damage plastic model for concrete failure. The plastic part is based on stress of the undamaged state of the material (named effective stress) and the damage part is based on total strains. The behaviour of concrete is elastic until the yield surface is reached. The initial damage threshold surface is identical to the shear yield surface. This kind of concrete model is widely used because plasticity and damage are simply coupled and it mathematically leads to

a well posed problem. Furthermore, calibration procedure of parameters is relatively easy to deal with.

Experiments show an increase of concrete strength as strain rate increases, both in tension and in compression. In the model described here, this phenomenon is taken into account as follows: plasticity is replaced by viscoplasticity to allow stress state to lie outside the yield surface and damage rate is bounded to produce a viscous regularization.

1.1 Elasto-viscoplastic formulation

The elasto-viscoplastic formulation is an extension of the commonly used Duvaut-Lions model described in [3]. Simo postulated that the elasto-viscoplastic strain rate is given by:

$$\dot{\varepsilon}^{vp} = C^{-1} : \frac{1}{\eta}\left(\sigma^{vp} - \sigma^{ep}\right) \tag{1}$$

where he introduced η called the "fluidity parameter" (physically, η is a time constant which could be related to crack propagation). σ^{ep} is the elastoplastic stress and σ^{vp} the elasto-viscoplastic stress, and C the Hooke's tensor. The viscoplastic stress rate:

$$\dot{\sigma}^{vp} = C : \left(\dot{\varepsilon} - \dot{\varepsilon}^{vp}\right) = C : \dot{\varepsilon} - \frac{1}{\eta}\left(\sigma^{vp} - \sigma^{ep}\right)$$

is replaced by the first order accurate formulae thanks to an Euler backward scheme:

$$\frac{\Delta\sigma^{vp}_{n+1} - \Delta\sigma^{vp}_{n}}{\Delta t} = C : \frac{\Delta\varepsilon}{\Delta t} - \frac{1}{\eta}\left(\sigma^{vp}_{n+1} - \sigma^{ep}_{n+1}\right) \tag{2}$$

where Δt is the current time step.

From which we finally obtain:

$$\sigma^{vp}_{n+1} = \frac{\sigma^{vp}_{n} + C : \Delta\varepsilon + \frac{\Delta t}{\eta}\sigma^{ep}_{n+1}}{1 + \frac{\Delta t}{\eta}} = \frac{\eta\sigma^{vp}_{trial} + \Delta t\sigma^{ep}_{n+1}}{\eta + \Delta t} \tag{3}$$

Then, the next step is to provide a fit between the fluidity coefficient η and the strain rate. The fluidity coefficient η varies with strain rate according to the generic expression below:

$$\eta = \eta_{0i}(\hat{\dot{\varepsilon}} / \dot{\varepsilon}_{0i})^{-n_i} \tag{4}$$

where n_i, η_{0i}, $\dot{\varepsilon}_{0i}$ are input parameters and $\hat{\dot{\varepsilon}}$ is a measure of the strain rate defined as follows:

$$\hat{\dot{\varepsilon}} = Max(\dot{\varepsilon}^{d}, \dot{\varepsilon}_{V} / 3) \tag{5}$$

where :

$$\dot{\varepsilon}^{d} = \frac{\varepsilon^{d}_{n+1} - \varepsilon^{d}_{n}}{\Delta t}$$

$$\dot{\varepsilon}_V = (tr\Delta\varepsilon)/\Delta t$$

with $\varepsilon_i^d = \sqrt{\frac{1}{2}\left[\left(\varepsilon_{xx}-\varepsilon_{yy}\right)^2+\left(\varepsilon_{yy}-\varepsilon_{zz}\right)^2+\left(\varepsilon_{zz}-\varepsilon_{xx}\right)^2+6(\varepsilon_{xy}^2+\varepsilon_{yz}^2+\varepsilon_{xz}^2)\right]_i}$ $\quad i\in[n,n+1]$

ε_i^d is a measure of the deviatoric strain rate and $\dot{\varepsilon}_V$ is the volumetric strain rate, the latter being introduced to have a strain rate in tri-tension.

Two distinct fluidity parameters are used: these are the fluidity parameters in uniaxial tensile stress η_t and uniaxial compressive stress η_c. η_t and η_c are defined according to equation (4), but with different input parameters for each.

$$\eta_t = \eta_{0t}\left(\dot{\hat{\varepsilon}}/\dot{\hat{\varepsilon}}_0\right)^{-n_t} \quad \eta_c = \eta_{0c}\left(\dot{\hat{\varepsilon}}/\dot{\hat{\varepsilon}}_0\right)^{-n_c} \tag{6a&b}$$

In both cases, $\dot{\hat{\varepsilon}}_0$ is chosen equal to 1 s^{-1}. Default values of the four parameters: η_{0t}, η_{0c}, n_t and n_c have to be identified on experimental correlations of Dynamic Increased Factors.

For triaxial stress cases, the fluidity parameter η used in equation (3) is interpolated between tensile and compressive fluidity parameters as a function of the viscoplastic stress triaxiality $T_x^{vp} = J_1/\sqrt{3J_2}$ as follows:

$$\eta = (1-H(T_x^{vp}))\left[\eta_t + \min(1,\langle -T_x^{vp}\rangle)(\eta_c-\eta_t)\right] + H(T_x^{vp})\eta_t \tag{7}$$

when $-1 < T_x^{vp} < 0$. $\langle X\rangle = X \; if \; X>0, else \; 0$ is the Macaulay brackets and H is the Heaviside function.

1.2 The bounded rate model

The bounded rate model is described in [2]. From a physical point of view, the basic idea is that the damage rate is finite because the cracking process is not instantaneous (the crack velocity is finite) and from a mathematical point of view it was demonstrated that the problem remains well posed as long as damage rate is bounded and the damage is not too close to 1.

The damage rate $\dot{d}$ is asymptotically bounded thanks to the following expression:

$$\dot{d} = \dot{d}_\infty\left(1-e^{-b\langle d^s-d\rangle}\right) \tag{8}$$

where: $\dot{d}_\infty$ stands for the maximum damage rate, d^s is the static damage i.e. calculated without rate effect, d is the damage and b is a parameter.

When the argument of the exponential term is much smaller than one, the damage rate can be approximated by:

$$\dot{d} \simeq b\dot{d}_\infty\langle d^s-d\rangle = \frac{\langle d^s-d\rangle}{\mu} \tag{9}$$

This formula is that provided by simple delay damage model; see for example [4]. Expression (9) shows that the product $b\dot{d}_\infty$ is the inverse of a time constant μ. As shown by parametrical studies, it was important to maintain this product constant so b is replaced by μ that turns to be the new parameter of the model.

Implementation of the model is easy. First, the time derivative of (8) is calculated and expressed as follow:

$$\ddot{d} = b(\dot{d}_s - \dot{d})(\dot{d}_\infty - \dot{d})$$

Then, as in viscoplasticity, an Euler backward scheme leads to the first order accurate formulae:

$$\frac{\dot{d}_{n+1} - \dot{d}_n}{\Delta t} = b(\dot{d}^s_{n+1} - \dot{d}_{n+1})(\dot{d}_\infty - \dot{d}_{n+1}) \tag{10}$$

So, it remains to solve the second order equation:

$$\dot{d}^2_{n+1} - \left(\dot{d}_\infty + \dot{d}^s_{n+1} + \frac{1}{b\Delta t}\right)\dot{d}_{n+1} + \dot{d}^s_{n+1}\dot{d}_\infty + \frac{\dot{d}_n}{b\Delta t} = 0$$

from which the solution gives an explicit expression of damage rate at each time increment:

$$\dot{d}_{n+1} = \frac{1}{2}\left((\dot{d}_\infty + \dot{d}^s_{n+1} + \frac{1}{b\Delta t}) - \sqrt{(\dot{d}_\infty + \dot{d}^s_{n+1} + \frac{1}{b\Delta t})^2 - 4(\dot{d}^s_{n+1}\dot{d}_\infty + \frac{\dot{d}_n}{b\Delta t})}\right) \tag{11}$$

Damage at time step $n+1$ is finally obtained by integrating the damage rate over the time step:

$$d_{n+1} = d_n + \dot{d}_{n+1}\Delta t \tag{12}$$

Brittle damage accumulation law is given by the linear law:

$$d^s(\tau) = d_{max}A^{bs}(\tau - \tau_0) \; for \; \tau \le \tau_{\max} \mid A^{bs}(\tau_{\max} - \tau_0) \le 1 \tag{13}$$

Brittle fracture energy is equal to the area under the stress-displacement curve after reaching the strength in tension and that gives the value of the shape parameter A^{bs}:

$$A^{bs} = \frac{\tau_0 L_{ch}}{2G^b_f} \tag{14}$$

where L_{ch} is the 'crack band width' of the integration domain also called the concrete characteristic length. Thanks to an equivalent interpretation due to [5], this parameter is the ratio of the specific energy per unit of volume g^b_f dissipated during the deformation to the fracture energy per unit of area G^b_f:

$$L_{ch} = G^b_f / g^b_f \tag{15}$$

Within this model, damage is no longer localized in a single element but is spread over the concrete characteristic length. In [6], authors proposed to choose L_{ch} within the range $\left[3D_{agg}, 5D_{agg}\right]$ where D_{agg} is the maximum aggregate size. Nevertheless, there is no consensus on this subject. For example, in [7], when studying calibration of concrete model on three sizes of concrete beams, the author obtained the better fit with a much larger value (x3). So, L_{ch} is a parameter of the model to be calibrated such as μ and $\dot{d}_{\infty}$.

With increasing deformation rate, damage is spread out over a larger band than L_{ch}. Of course, the size of the mesh should be such that several elements are inside the band in order to have an adapted discretization (see Figure 3). Conversely, with decreasing deformation rate, damage is localized on a narrow band. Therefore a very fine mesh is required to avoid mesh dependency and, in practice, if the strain rate is too low, the bounded rate model is ineffective to regularize. Indeed, parametric studies have shown that regularization is obtained only when the following condition: $\dot{d}^s > \dot{d}_{\infty}$ is fulfilled.

To avoid introducing a new parameter, μ could be taken as the fluidity parameter η which is consistent with the definition of the shifted damage threshold (eq. 9). The fluidity parameter η is nevertheless not constant but as it varies more slowly than damage, the previous implementation of the model is still relevant.

3 EVALUATION TESTS

After a single element test used to check the implementation of the bounded rate model within the DPDC constitutive law, two other tests are presented: the first one is an indirect tension test and the second a three-point bending test on an impacted notched beam.

3.1 Single element test

A cubic element is loaded in uniaxial tension along the z axis with a constant strain rate $\dot{\varepsilon}_{zz}$ = 100 s^{-1}. Default parameters values are used for the bounded rate model: L_{ch} = 0.01 m and $\dot{d}_{\infty} = 10^4$ s^{-1}. The element length of the cube is L = 0.001 m, one tenth of L_{ch}.

For this simple case, the initial damage threshold and the current thresholds read:

$$\tau_0^b = \left[\sqrt{E}\varepsilon_{\max}^{princ}\right]_{\text{when the shear failure is reached at } t=t_p \text{ and } \varepsilon_{\max}^{princ}>0} = \sqrt{E}\dot{\varepsilon}_{zz}t_p$$

$$\tau^b = \sqrt{E}\varepsilon_{max}^{princ} = \sqrt{E}\dot{\varepsilon}_{zz}t$$

Then, the static damage is given by equations (13) and (14):

$$d^s(\tau) = d_{max}A^{bs}(\tau-\tau_0) = \frac{\tau_0 L_{ch}}{2G_f^b}\sqrt{E}\dot{\varepsilon}_{zz}(t-t_p) = \frac{f'_t L_{ch}}{2G_f^b}\dot{\varepsilon}_{zz}(t-t_p) \; for \; t > t_p$$

from which the static damage rate is deduced: $\dot{d}^s(\tau) = \frac{f'_t L_{ch}}{2G_f^b}\dot{\varepsilon}_{zz}$. The numerical application

gives: $\dot{d}^s(\tau) = 2.64\ 10^4\ s^{-1}$ in agreement with the calculation as can be verified on Figure 1 showing static and dynamic damage. The third parameter: $\mu = \eta$ affects the nonlinear part of the dynamic damage evolution (until the maximum damage rate is reached).

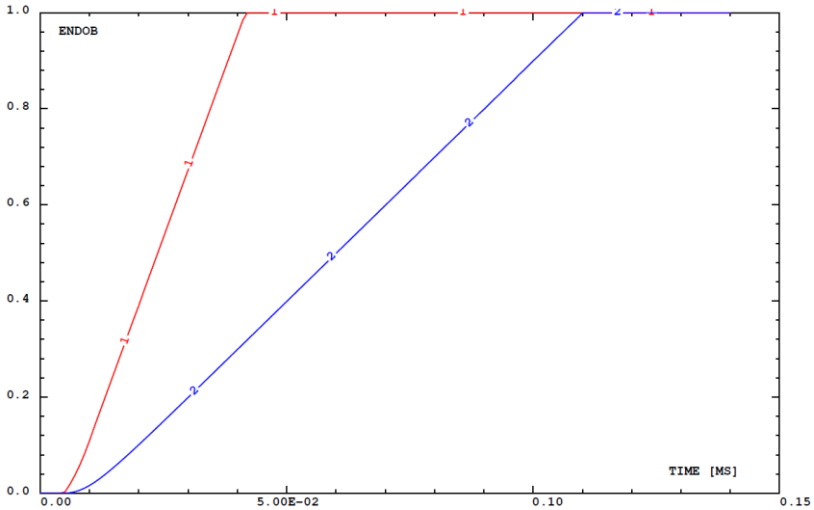

Figure 1: Static damage (in red) and dynamic damage (in blue) for tension loading at a strain rate $\dot{\varepsilon}_{zz}$ = 100 s^{-1}.

Stress time histories σ_{zz}(t) within the bounded rate model are plotted on Figure 2. It can be seen that the transition between hardening and softening is smooth which is favorable to avoid localization.

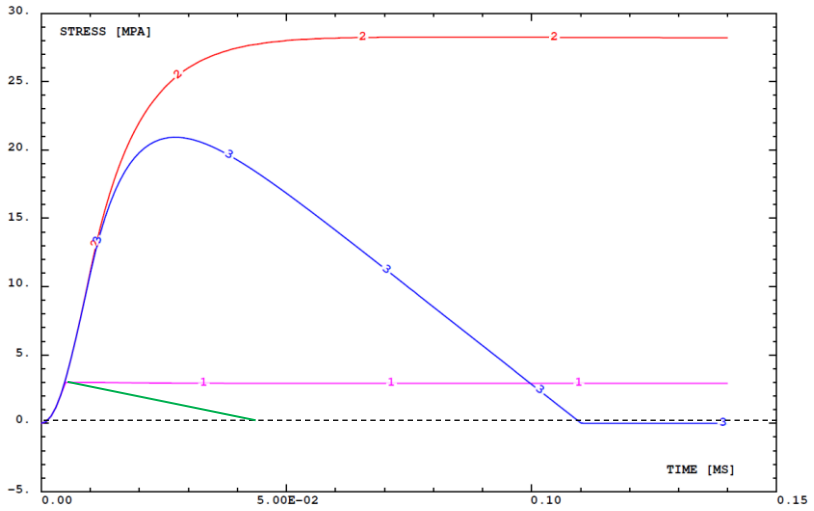

Figure 2: Stress time histories for a tension test at a strain rate $\dot{\varepsilon}_{zz}$ = 100 s^{-1}.
(Plastic stress is colored in pink, viscoplastic stress in red, final stress in blue and final static stress in green.)

3.2 Dynamic Brazilian test

The test in tension is a Brazilian one in which a vertical compressive load is applied diametrically to a cylindrical specimen by mean of two thin strip bearings between the sample and the steel plates. The cylinder is 7 cm high and 7 cm in diameter (B = 7 cm, D = 7 cm). The mean element size is 1.25 mm. The characteristic data used for concrete are: E_c = 26.4 GPa, ν_c = 0.2, ρ_c = 2400 kg/m^3, f'_c = 30 MPa and $Dagg$ = 1.0 cm. All others parameters are default values given by the DPDC model, so f'_t = 3 MPa, L_{ch} = 1 cm and $\dot{d}_\infty = 10^4$ s^{-1}.

The bearings are modelled with an elastic material whose elastic properties are the same as the concrete. Perfect bond is assumed between the bearings and the specimen. The bottom steel plate is blocked and the upper one moved downward with a speed of 20 cm/s.

To study mesh bias, the mesh is not aligned with the crack, but is rotated by about thirty degrees counter-clockwise.

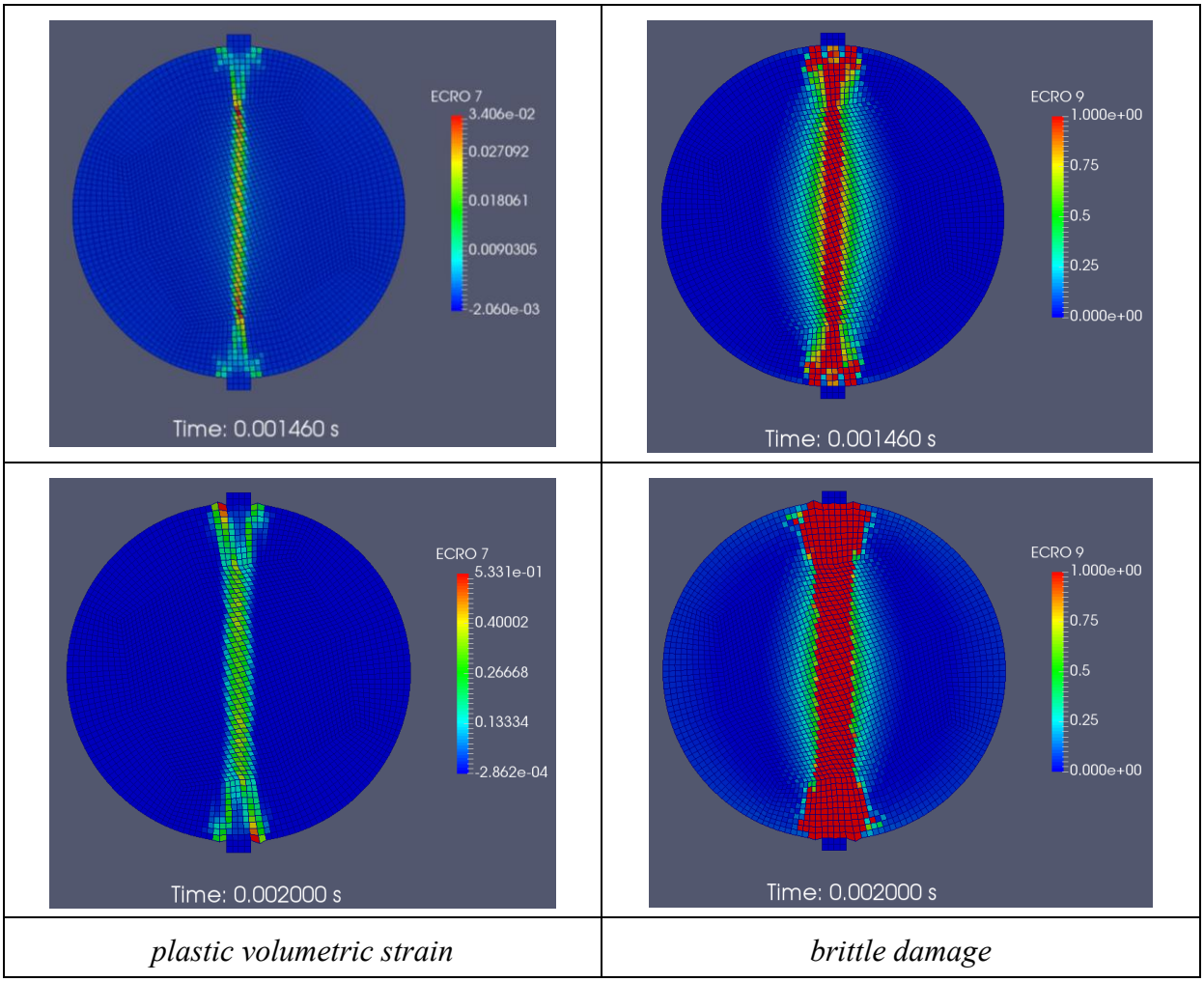

Figure 3: Damage patterns for the Brazilian test.

The plastic volumetric strain which is a good marker of cracks, and the brittle damage are plotted on Figure 3. It can be seen that both are vertical so no mesh bias is noticeable.

The first instant is the one for which damage reached one along the entire vertical plane. Damage is not localized but varies smoothly within a vertical band. At the end of the simulation, this is no longer true, because the complete damaged zone (where d^b =1, in red on Figure 3) has gained ground on the intermediate damaged zone. Simultaneously, the crack width has increased.

Vertical force time history and equivalent tension stress versus vertical displacement of bearings are drawn on Figure 4. The tensile stress decreases toward zero without any artificial rebound. The simulation gives σ_t = 5.2 MPa and the dynamic increase factor is *DIF* = 1.73 in reasonable agreement with the tabulated values.

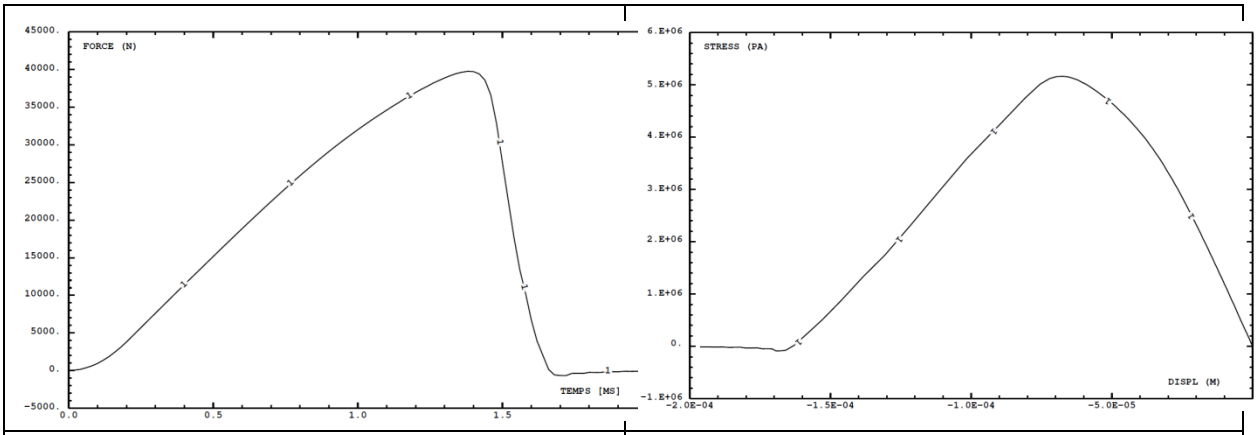

Vertical force time history | *Equivalent tension stress versus displacement*

Figure 4: Strengths obtained with the bounded rate model.

3.3 Dynamic three-point bending tests on notched beams

Zhang's results about the fracture behavior of high-strength concrete at a wide range of loading rates are used to test the bounded rate model [8]. Dynamic tests were performed with a drop-weight impact machine.

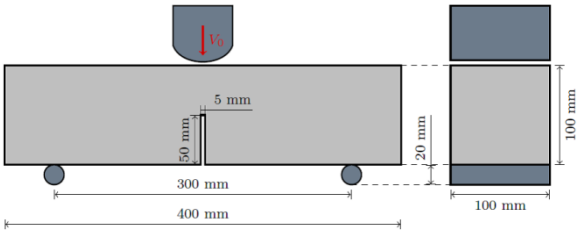

Figure 5: Geometry of specimen.

Three-point bending tests on notched beams were carried out as sketched on Figure 5 where the dimensions of the tested beam are given. The mass of the hammer is 120.6 kg.

Mechanical properties of concrete and steel for the hammer and the support rollers are gathered in Table 1 and Table 2 respectively. Here, the following values have been used: L_{ch} = 1 cm (the maximum size of aggregates is 1.2 cm) and $\dot{d}_{\infty}$ = 2 10^3 s^{-1}. These low values have been chosen to favor regularization and to fit with the highest velocity of the hammer.

Table 1: Mechanical properties of the high-strength concrete.

ρ (kg/m^3)	E (GPa)	ν	f_c (MPa)	f_t (MPa)	G_f (J/m^2)
2400.	43.3	0.18	105.	6.3	148.

Table 2: Mechanical properties of steel.

E (GPa)	ν
200	0.33

3.3.1 Mesh objectivity

Three element sizes are used for the meshes: L = 5 mm, L = 1.66 mm and L = 1 mm. Furthermore, to study mesh bias, the region of the mesh where the crack develops is not aligned with the crack, but is rotated by about thirty or seventy degrees clockwise. In these last cases, the element size is L = 1.66 mm.

Brittle damage and plastic volumetric strain obtained with the various meshes when the initial velocity of the hammer is V_{0ham} = 1.76 m/s are shown on Figure 6. In all cases, the brittle damage zone is almost the same whatever the size of the mesh and its orientation relative to the crack. Nevertheless, the plastic volumetric strain reveals two parallel cracks which is surprising. As the bifurcation occurs at the notch root, an area of stress concentration, the bounded rate model is suspected to be not suitable for zones of strong stress gradient.

Reaction force time histories and internal energy time histories are plotted on Figure 7. The results are not identical but the discrepancies introduced by the meshes seem reasonable.

3.3.1 Comparison with the experiments

Reaction forces are plotted against loading point displacement of the notched beams for the two highest velocities of the hammer (see Figure 8). Due to the fit, the agreement for the test with the highest velocity is good, but the agreement is lost for the other tests.

The maximum of reaction forces and the apparent fracture energies are gathered in Table 3. It can be verified that the accuracy of the results decreases with the loading rate. Consequently, a single set of coefficient $\dot{d}_{\infty}$ seems not able to reproduce strain rate effect.

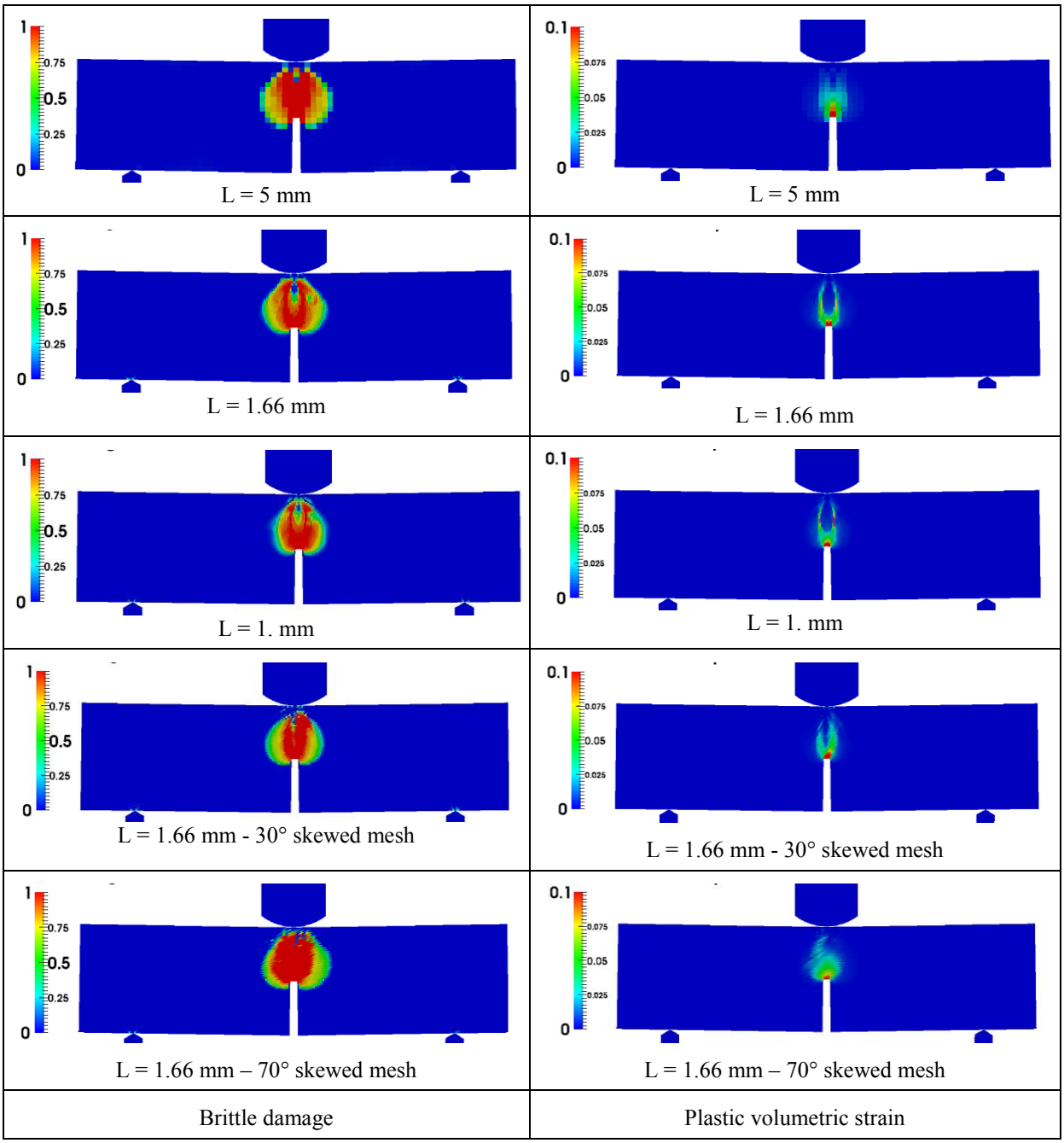

Figure 6: Damage patterns of the impacted notched beam – V_{0ham} = 1.76 m/s.

Table 3: Comparison between experiments and model.

V_{0ham} (m/s)	0.88	1.76	2.64		V_{0ham} (m/s)	0.88	1.76	2.64
Max. of reaction force (kN) - test	21.9	34.7	38.0		G_f (J) -test	6.0	16.8	33.6
Max. of reaction force (kN)- model	17.9	28.4	34.5		G_f (J) -model	6.9	18.4	32.4

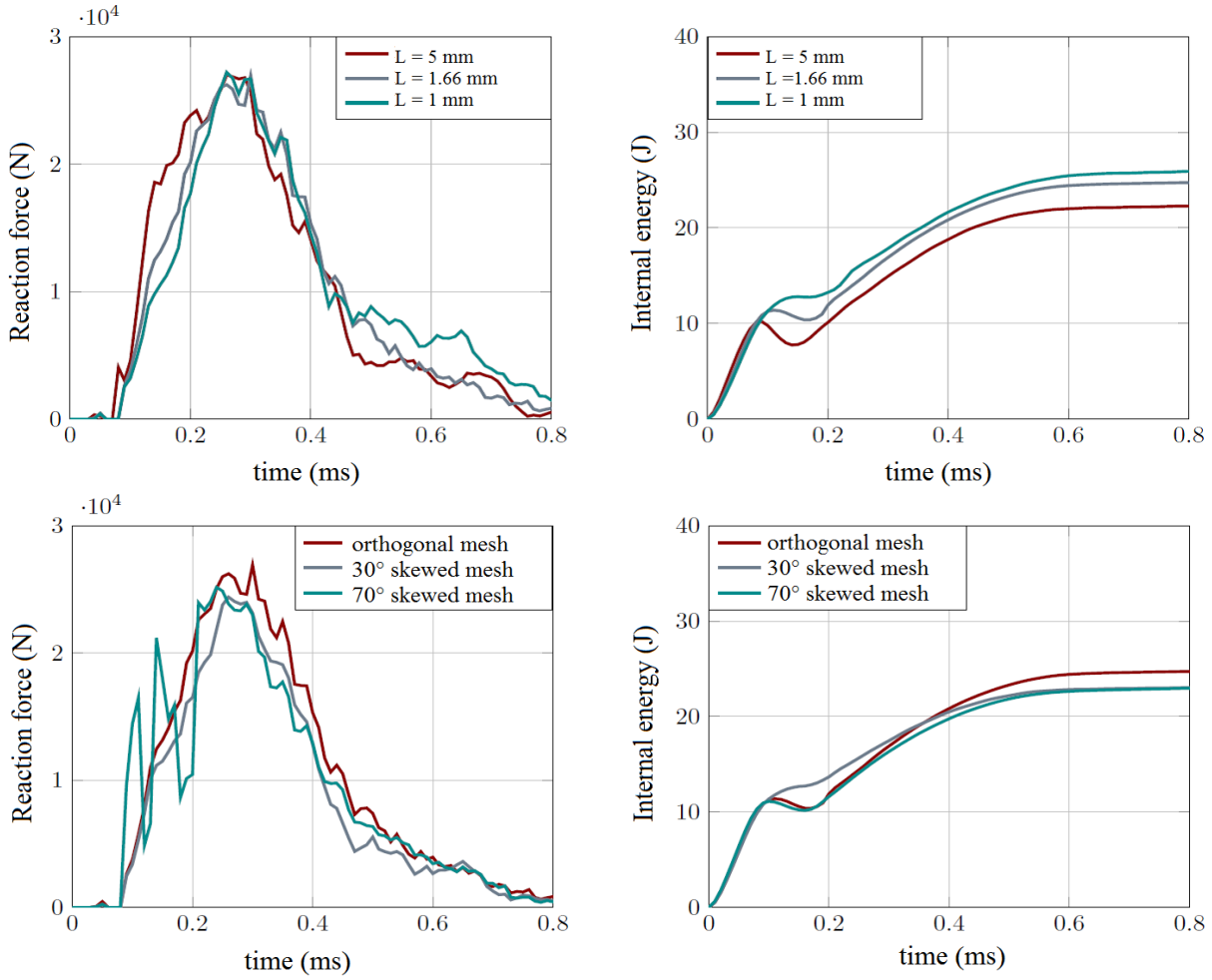

Figure 7: Reaction force and internal energy of the impacted notched beam – V_{0ham} = 1.76 m/s.

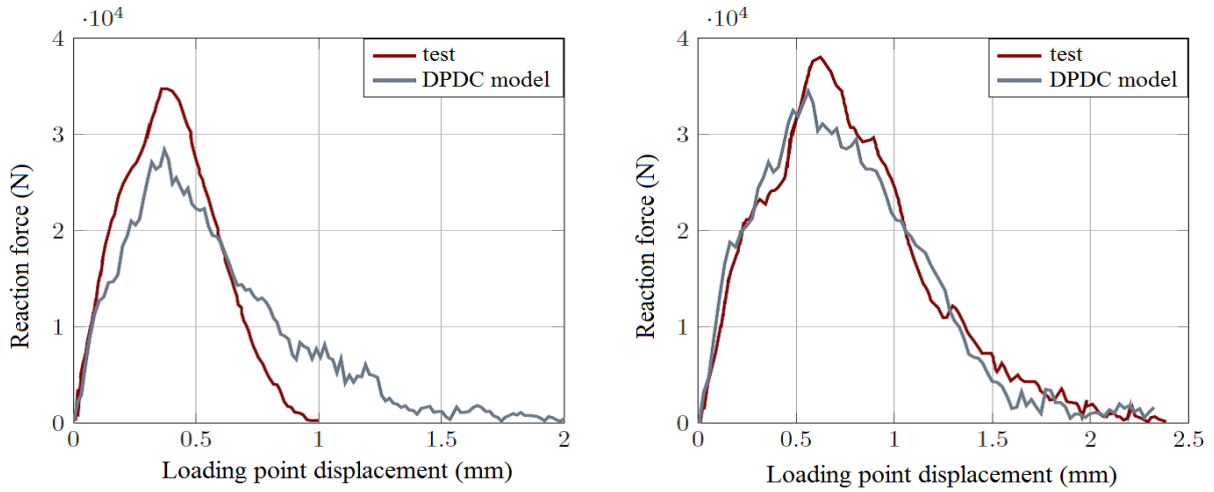

Figure 8: Reaction forces versus loading point displacement (left: V_{0ham} = 1.76 m/s, right: V_{0ham} = 2.64 m/s).

4 CONCLUSIONS

The model is very easy to implement because it leads to an explicit expression of the rate of damage at each time increment.

The new model has been verified on skewed mesh (relatively to crack) and compared to experimental results of the literature: an impacted notched beam [8] loaded at relatively moderate rates ($\simeq$ 1 m/s). It was shown that the bounded rate model regularizes deformations when the strain rate is larger than 1 s^{-1} and the mesh size about 1 mm. In that case, damaged zones are almost mesh-independent in size and orientation. Nevertheless, crack pattern revealed by the plastic volumetric strain is not satisfactory because it does not match with a single crack. So, the bounded rate model is suspected to be not suitable for zone of strong stress gradient such as notch tip.

Furthermore, calibration on these experiments has not led to a universal set of coefficients yet. So, a large amount of investigation remains to be done to broaden the loading rate range, to precise the lower bound rate that maintains regularization for a given mesh size, and to find a formulation with a single set of parameters.

REFERENCES

[1] D. Guilbaud, Damage plastic model for concrete failure under impulsive loadings, COMPLAS XIII (2015).
[2] O. Allix, The bounded rate concept: A framework to deal with objective failure predictions in dynamic within a local constitutive model, International Journal of Damage Mechanics 0(0), pp. 1-21, (2012).
[3] J.C. Simo, J.G. Kennedy, S. Govindjee, Non-smooth multisurface plasticity and visco-plasticity, loading / unloading conditions and numerical algorithms, Int. J. for Numerical Methods in Engineering, Vol. 26, pp. 2161-2185, (1988).
[4] A. Genikomsou, M. A. Polak , Finite element analysis of punching shear of concrete slabs using damaged plasticity model in ABAQUS, Engineering Structures 98, pp. 38-48, (2015).
[5] J. Oliver, A consistent characteristic length for smeared cracking models, Int. J. for Numerical Methods in Engineering, vol. 28, pp. 461-474, (1989).
[6] Z.P. Bazant and G. Pijaudier-Cabot, Measurement of the characteristic length of non-local continuum, J. of Engineering Mechanics, ASCE, Vol. 115, pp.755-767, (1989).
[7] Dubé J.F., Identification des paramètres d'un modèle de comportement pour les structures en béton, Mémoire d'Habilitation à Diriger les Recherches, Université de Montpellier II, (2005).
[8] X. Zhang, G. Ruiz, R. Yu and M. Tarifa, Fracture behavior of high-strength concrete at a wide range of loading rates, International Journal of Impact Engineering, 36(10-11), pp. 1204-1209, (2009).